Proceedings of the ASME 2010 3rd Joint US-European Fluids Engineering Summer Meeting and
8th International Conference on Nanochannels, Microchannels, and Minichannels
FEDSM-ICNMM2010
August 1-5, 2010, Montreal, Canada

FEDSM-ICNMM2010-30398

DROPLET FORMATION BY DRIPPING AT MICRO T-JUNCTION IN LIQUID-LIQUID MIXING

Sujin Yeom
Department of Mechanical Engineering, KAIST
Daejeon, Republic of Korea

Sang Yong Lee
Department of Mechanical Engineering, KAIST
Daejeon, Republic of Korea

ABSTRACT

In the present work, the phenomenon of droplet formation by dripping at a micro T-junction in liquid-liquid mixing was studied experimentally.

The drop formation process consisted of three stages: the X-Y growth, X growth, and the detachment stages. In the X-Y growth stage, the bulged part of the disperse phase grows both in X (parallel to the main channel) and Y (lateral to the main channel) directions. The X-Y growth stage is followed by the X growth stage where the bulged part grows only in the main channel direction. Subsequently, in the detachment stage, the drag force exerted by the continuous phase becomes larger than the surface tension force between the two phases and the bulged part is finally separated into a droplet with regular intervals through a rapid necking process.

Droplet sizes were estimated from the drop generation frequency and the flow rate of the disperse phase, and were also confirmed by direct measurements through photography. The sizes of the micro droplets generally decrease with the larger flow rate of the continuous phase or with a smaller flow rate of the disperse phase. This is due to the increase of the interfacial shear force between the two phases through the increase in the relative velocity. The droplet size also decreases with increase of the viscosity of the either phase. This again is due to the increase of the interfacial shear force (and hence the drag force) between the phases when the viscosity of either phase becomes large. The measured drop sizes will serve as a set of the bench-marking data for the development of a droplet detachment model in the dripping mode at micro T-junctions.

NOMENCLATURE

Symbol	Description	Unit
D	Droplet diameter	m
j	Superficial velocity	m/s
L	Size of the bulged part in X-direction	m
S	Size of the bulged part in Y-direction	m
t	Time	s
μ	Viscosity	Pa·s
ρ	Density	kg/m^3
σ	Interfacial tension	N/m
	Subscripts	
c	Continuous phase fluid	
d	Disperse phase fluid	
E	End of X growth stage	

INTRODUCTION

Recently, there have been numerous studies on the liquid micro-droplet formation to control size and uniformity of the droplets for the application to a lab-on-a-chip system, the synthesis of microparticles, and other uses [1-4]. The droplet formation methods can be grouped into three categories: coflow method [5], flow focusing method [6], and crossflow method [7, 8]. The flow focusing method generates droplets only with limited geometrical configurations [8]. By comparing previous researches [9, 10] in which the crossflow method and the coflow method were applied to generate bubbles, it was confirmed that the crossflow method stably generates bubbles in larger velocity ranges than the coflow method under similar operation conditions. Among the three methods above, the crossflow method is most suitable for generating droplets with wide ranges of velocity and pressure. Therefore, a number of studies have been performed on droplets formation using the crossflow method (or T-junction) [3-5].

Figure 1 shows the droplets formation method using a T-junction. The droplets are formed by the differences in the fluid properties and the flow characteristics (such as flow orientations and velocities) between the disperse and the continuous phases. Here, the disperse phase and the continuous phase are injected through the side and the main inlets, respectively. Depending on

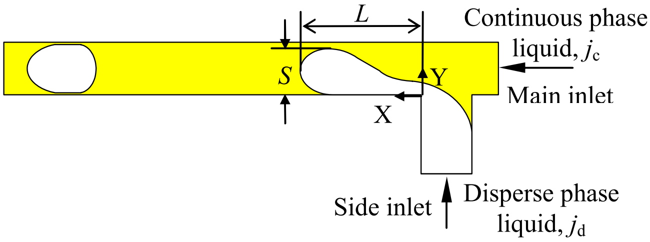

Figure 1: Schematic view of droplet formation at a T-junction

the velocity of both phases, three different modes of the droplet formation were reported: squeezing, dripping, and jetting [11]. Figure 2(a) shows droplets formed by squeezing. In the squeezing mode, the disperse phase blocks the main channel and the droplet is formed by the build-up pressure at the upstream of T-junction. This mode occurs at a low velocity of both phases and the droplets are highly uniform in sizes but always larger than the channel diameter. Figure 2(b) shows droplets formed by dripping. In this mode, droplets are formed by the shear stress exerted by the continuous phase on the interface between the fluids. This mode appears at a low velocity of the disperse phase and a high velocity of the continuous phase. Unlike the squeezing mode, the disperse phase does not block the main channel during the droplet formation process. Droplets formed by dripping are also highly uniform in sizes and various sizes are available. In the jetting mode, as shown in Figure 2(c), droplets are formed by the instability at the interface between the fluids. Jetting occurs at high velocities of both phases, and the formed droplets are generally not uniform. Based on these observations, the dripping mode is most likely suitable for the generation of uniform micro-droplets.

There have been many studies on micro-droplets formation by dripping. Thorsen et al. [12] derived a simple relationship to predict the droplet size by equating the shear force and Laplace pressure. Van der Graaf et al. [13] simulated the droplet formation process using the Lattice Boltzmann method and compared their results with the experimental results of Xu et al. [14]. De Menech et al. [11] reported that the droplet size decreases with a smaller viscosity ratio (μ_d/μ_c) and a larger capillary number ($\mu_c j_c/\sigma$) through a numerical simulation. Husny et al. [15] studied the effect of viscosity of the disperse and the continuous phases ranging from 1 to 6 mPa·s and 5 to 50 mPa·s, respectively, on the droplet size. They reported that the droplet size decreases with increasing of the viscosity of the either phase. They also proposed a correlation to predict the droplet size by equating the surface tension force and the drag force but the correlation does not represent the experimental data with satisfaction. Xu et al. [14] also proposed a correlation to predict the droplet size by balancing the surface tension force to the drag force, but the effect of the disperse phase viscosity was not taken into account.

Despite of many studies on the droplets formation by dripping, quantitative data pertaining to the droplet sizes are still lacking, which is essential to develop correlations for prediction of the micro droplet size. Therefore, in this paper, the droplet formation process by dripping was examined and then the droplet sizes were measured carefully (to be used as the bench-marking data) with the viscosity and the superficial velocity of both fluids taken as the primary parameters.

EXPERIMENTS

Figure 3 shows the experimental setup for generation of the micro-droplets. A micro T-junction was fabricated by soft lithography by PDMS (Poly-Di-Methyl-Siloxane, Sylgard184, Dow Corning). It has the square cross-sections with their sides being 90 µm with an error tolerance of 5 µm.

Four combinations of the working fluid were tested, which were previously adopted by Tice et al. [16]. The interfacial tensions were kept about the same and only the viscosities were varied, as listed in Table 1. (Note that the effect of the interfacial tension was not studied in the present work.

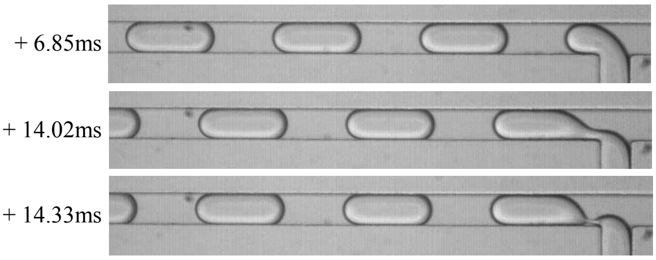

(a) Squeezing
($\mu_c = 2.3 \times 10^{-3}$ Pa·s, $\mu_d = 2.7 \times 10^{-3}$ Pa·s,
$j_d = 0.021$ m/s, $j_c = 0.021$ m/s)

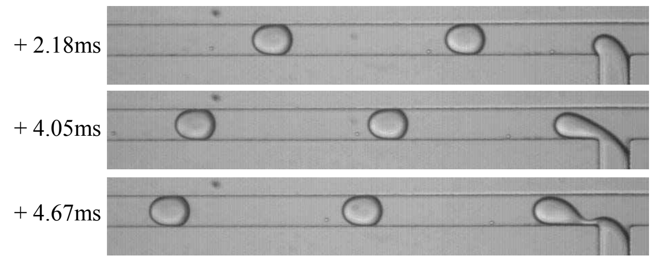

(b) Dripping
($\mu_c = 2.3 \times 10^{-3}$ Pa·s, $\mu_d = 2.7 \times 10^{-3}$ Pa·s,
$j_d = 0.021$ m/s, $j_c = 0.144$ m/s)

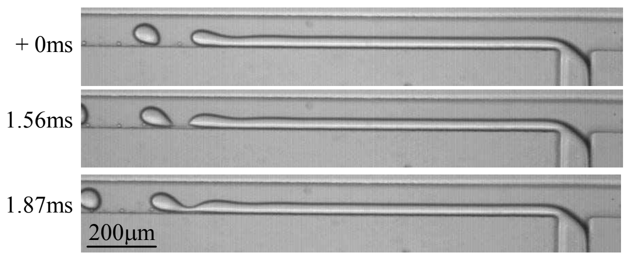

(c) Jetting
($\mu_c = 18 \times 10^{-3}$ Pa·s, $\mu_d = 19 \times 10^{-3}$ Pa·s,
$j_d = 0.014$ m/s, $j_c = 0.123$ m/s)

Figure 2: Droplet formation modes

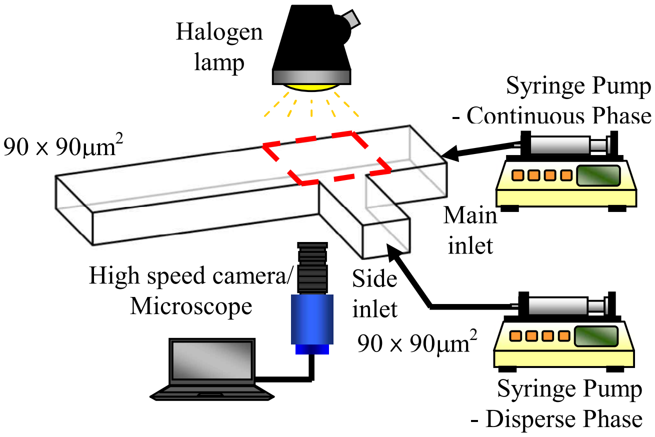

Figure 3: Experimental setup

However, it is known that the droplet sizes decrease as the interfacial tension decreases [7]). Case A represents a condition in which the viscosities of the both fluids (phases) are low and taken as the reference condition. Then, either the viscosity of the dispersed phase (case B) or the continuous phase (case C) was raised with the viscosity of the other phase being fixed. Finally, case D is for high viscosities in both phases. All the experiments were conducted under the temperature condition of 24 ± 2 °C that corresponds to the viscosity error range of 0.3 mPa·s.

The flow rate of the fluids was controlled using a syringe pump (KDS2100, KD Scientific) with an error tolerance of 1%. The disperse and the continuous phases were injected respectively through the side inlet in the range of 0.002-0.052 m/s and through the main inlet in the range of 0.02-0.17 m/s. The droplet formation process was examined in every case using a microscope (CKX-41, Olympus) and a high speed camera (X-streamVision XS-3, IDT Co. Ltd.) at 3210 frames per second with an exposure time of 30 µs. The volume of each droplet could be estimated by dividing the flow rate of the disperse phase by the number of droplets counted (per unit time), and was converted to the diameter assuming the spherical shape.

Table 1: Working fluids

Case	Disperse fluid	Continuous fluid (Volume mixture)	Viscosity x 10³ (Pa·s) μ_d	Viscosity x 10³ (Pa·s) μ_c	Density (kg/m³) ρ_d	Density (kg/m³) ρ_c	σ x 10³ (N/m)
A	Glycerol/ Water 24wt%	PFO/FC-3283 (1: 10)	2.7	2.3	1000	1820	10.6
B	Glycerol/ Water 64wt%		19				13.4
C	Glycerol/ Water 24wt%	PFO/PPP (1:10)	2.7	18		2030	11.4
D	Glycerol/ Water 64wt%		19				10.9

Criterion by	Flow patterns		
Tice et al.[16]	Plugs		Threshold
De Menech et al.[11]	Squeezing	Dripping	-
Symbols	□	■	○

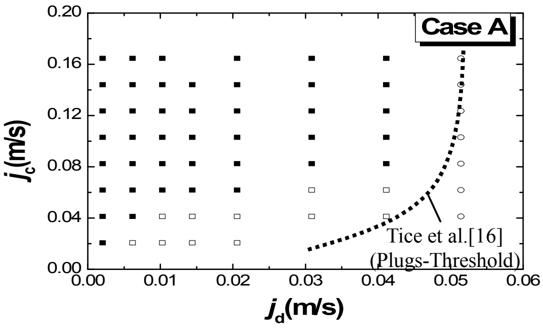

(a) Case A (μ_c = 2.3 x 10^{-3} Pa·s, μ_d = 2.7 x 10^{-3} Pa·s)

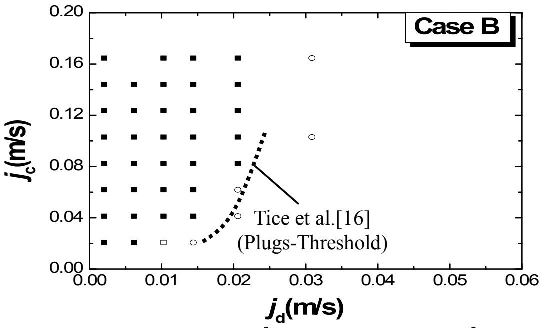

(b) Case B (μ_c = 2.3 x 10^{-3} Pa·s, μ_d = 19 x 10^{-3} Pa·s)

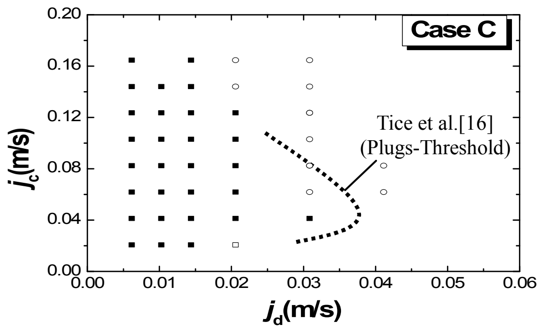

(c) Case C (μ_c = 18 x 10^{-3} Pa·s, μ_d = 2.7 x 10^{-3} Pa·s)

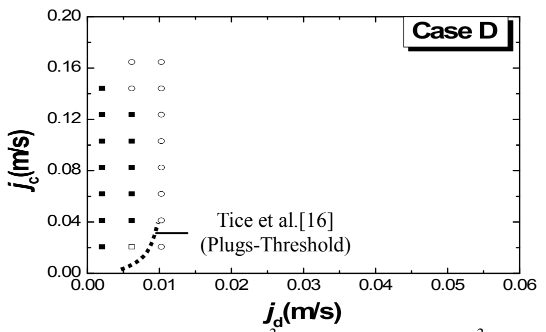

(d) Case D (μ_c = 18 x 10^{-3} Pa·s, μ_d = 19 x 10^{-3} Pa·s)

Figure 4: Droplet formation mode regime map

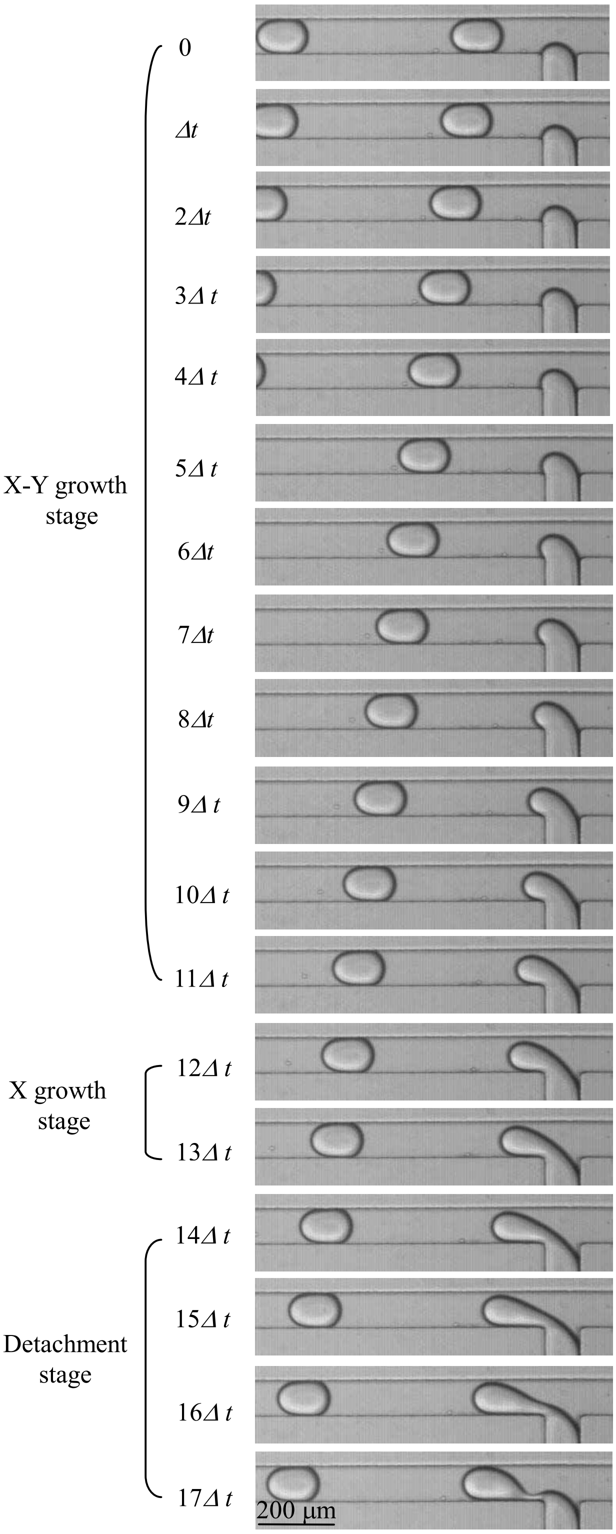

Figure 5: Droplet formation process by dripping (case A) (j_d = 0.021 m/s, j_c = 0.103 m/s, Δt = 3.115 x 10^{-4} s)

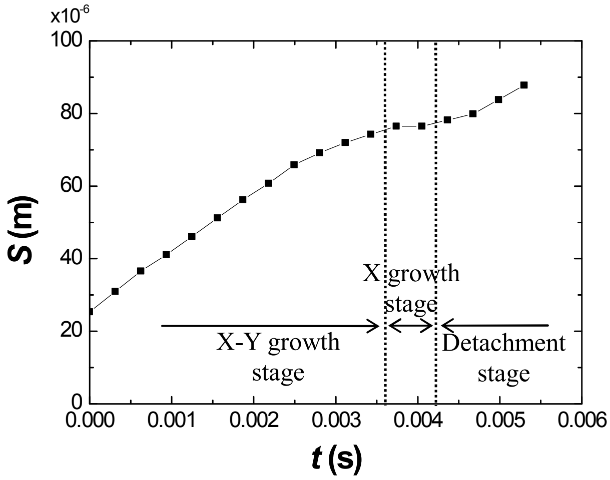

Figure 6: Droplet growth stages (j_d =0.021 m/s, j_c =0.103 m/s)

RESULTS

Droplet formation process

To confirm the conditions of dripping and to check the reliability of the experiments, comparisons were made with the droplet formation mode reported by Tice et al. [16] as shown in Figure 4. Tice et al. conducted experiments using a square T-junction with the cross sections of both the main and the side inlets being 50 x 50 μm^2. Drop formation process was categorized as plugs, threshold, and laminar modes. (As already mentioned in the introduction part, De Menech et al. [11] also classified the drop formation process into three modes, but in a slightly different way: squeezing, dripping, and jetting. Here, the squeezing and the dripping modes belong to the plugs mode, and the jetting mode is equivalent to the laminar mode. The transition regime between the dripping and the jetting modes corresponds to the threshold mode.) The dotted lines in Figure 4

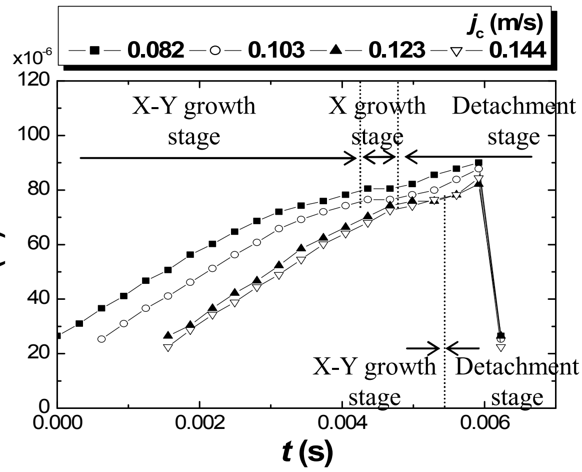

Figure 7: Droplet growth in Y-direction with time for case A (j_d =0.021 m/s)

represent the transition boundaries between the plugs and the threshold modes by Tice et al. In this paper, their boundaries were replotted in the j_d-j_c planes for easy comparison. Note that the present work covers wider experimental ranges than those of Tice et al. It was confirmed that, in general, the droplet formation regimes approximately well matches with the results of Tice et al.

Figure 5 shows an example of the droplet formation process by dripping at the micro T-junction for case A. The process is divided into three stages: the X-Y growth, X growth, and the detachment stage. The same behavior was observed for other cases. As evidenced by the figure, before the droplet detachment, the bulged part of the disperse phase does not block the main channel. The values of S, defined in Figure 1, were measured from each frame of Figure 5 and plotted in Figure 6. It can be clearly seen that, in the X-Y growth stage, the bulged part grows in X (parallel to the main channel) and Y directions (normal to the main channel) simultaneously. When the bulged part reaches a certain size in Y direction, the X growth stage begins. At this stage, the bulged part grows only in X direction. After a while, the grown bulged part is pushed to the downstream of the main channel and broken up by necking at the T-junction, as shown in the detachment stage of Figure 5. In this stage, S increases again to minimize the surface area of the bulged part. As seen in Figures 5 and 6, the growth stage occupies most of the formation time, and the detachment stage requires a very short period compared to the growth stage. Therefore, it is likely that the droplet volume is determined at the end of the X growth stage.

Figure 7 shows variations of S with time for different superficial velocities of the continuous phase. As mentioned earlier, S increases continuously during the X-Y growth stage while remains constant during the X growth stage. This X growth stage was not obvious with a higher superficial velocity (of the continuous phase) because the duration of the droplet formation period is short and consequently the droplet sizes are

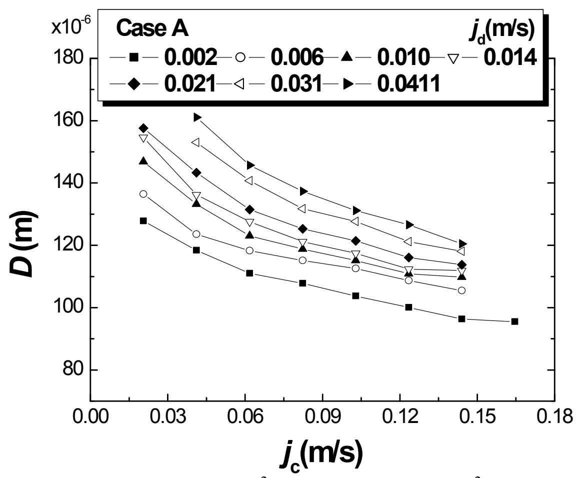

(a) Case A ($\mu_c = 2.3 \times 10^{-3}$ Pa·s, $\mu_d = 2.7 \times 10^{-3}$ Pa·s)

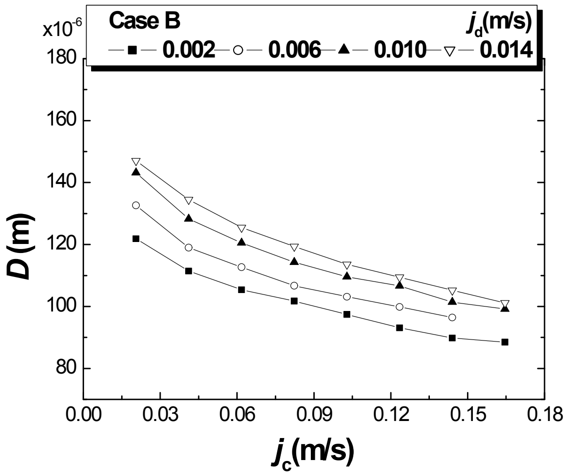

(b) Case B ($\mu_c = 2.3 \times 10^{-3}$ Pa·s, $\mu_d = 19 \times 10^{-3}$ Pa·s)

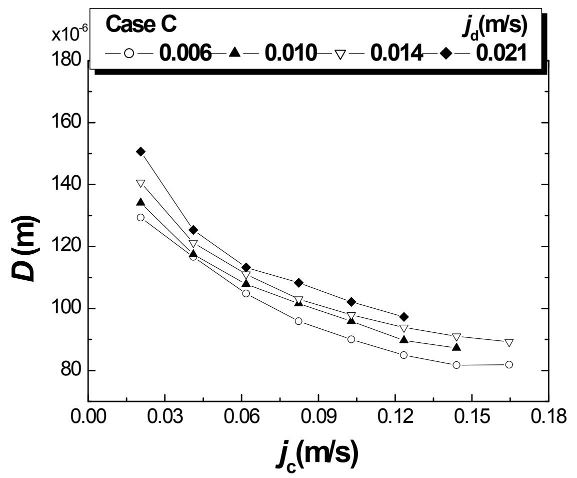

(c) Case C ($\mu_c = 18 \times 10^{-3}$ Pa·s, $\mu_d = 2.7 \times 10^{-3}$ Pa·s)

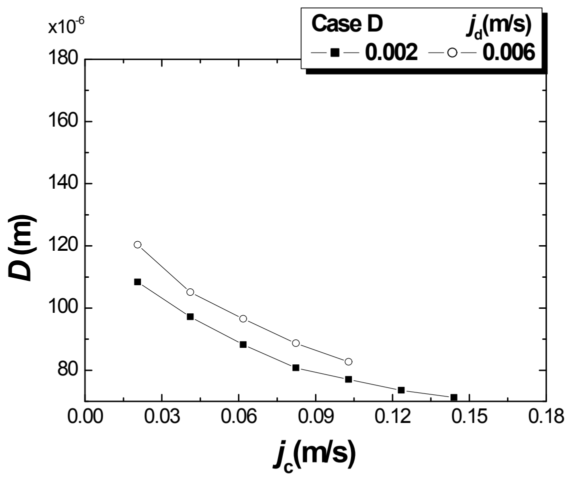

(d) Case D ($\mu_c = 18 \times 10^{-3}$ Pa·s, $\mu_d = 19 \times 10^{-3}$ Pa·s)

Figure 8: Variation of droplet diameter with velocity

small. In such a case, only an inflection point is observed and S increases thereafter until the bulged part is split off as a droplet.

Droplet diameter

Figure 8 shows quantitative data pertaining to the droplet size(equivalent diameter) with an error range of 2 μm. For fixed values of fluid viscosities, in general, the droplet size generally decreases with the larger superficial velocity of the continuous phase and/or with the smaller superficial velocity of the disperse phase. This is due to the increase of the interfacial drag (by the increase of the relative velocity) between the two phases. Such a tendency is consistent with that reported in the previous studies [7, 11].

Figure 9 shows the effect of the fluid viscosities on the droplet size. By comparing cases A and C with cases B and D, resectively, in which the viscosity of the continuous phase maintained the same, it is clear that the droplet size appears smaller with the higher viscosity of the disperse phase. This trend coincides with the results of Husney et al. [14]. This is due to the internal circulation behavior of the disperse phase induced by the continuous phase, as observed by Oishi et al. [17]. As the viscosity of the disperse phase increases, the internal circulation tends to be suppressed and consequently the drag force increases. Therefore, disintegration of the disperse phase is more enhanced. A similar phenomonon was reported by Clift et al. [18] for spherical liquid droplets. To examine the effect of the continuous phase viscosity, cases A and B were compared to cases C and D, respectively. The droplet size decreases as the viscosity of the continuous phase increases; this is again due to the increase of the drag force exerted by the continuous phase.

At this stage, it is meaningful to check the sensitivity of the droplet size to the viscosity of each phase. For example, for velocities of the disperse and the continuous phases being 0.006 m/s and 0.082 m/s, respectively, the droplet size decreases about 7-10% when the viscosity of the disperse phase is

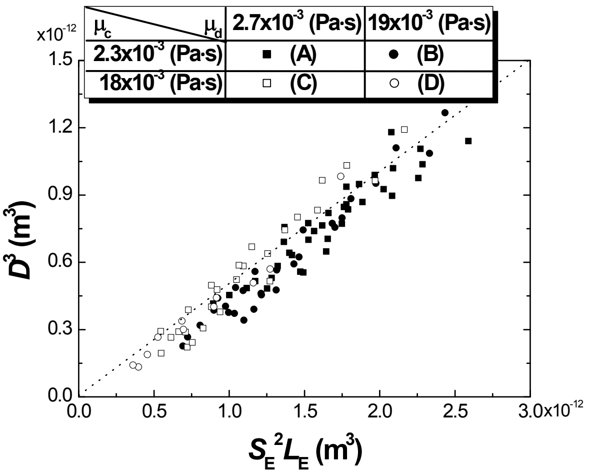

Figure 10: Relationship between D^3 and $S_E^2L_E$ at the end of the X growth stage

increased up to approximately 7 times (Compare points a and b in Figure 9.). When the viscosity of the continuous phase is increased by approximately 8 times (i.e., from points a to c in Figure 9.), the droplet size shows a decrease of nearly 17%. This implies that the droplet size is substantially influenced by the viscosity of the both phases, but more by the continuous phase viscosity.

As previously mentioned, it was posited that the size of the formed droplets is related to S at the end of the X growth stage. To verify this relationship, the dependence of D^3 on $S_E^2L_E$ was examined, which are proportional to the volume of the formed droplet and the volume of the bulged part at the end of the X growth stage, respectively. (Referenced to Figure 1, S_E and L_E denote the sizes of the bulged part in the X and Y directions, respectively, at the end of the X growth stage.) Figure 10 confirms a proportional relationship between D^3 and $S_E^2L_E$. Hence, the droplet volume at the end of the X growth stage may

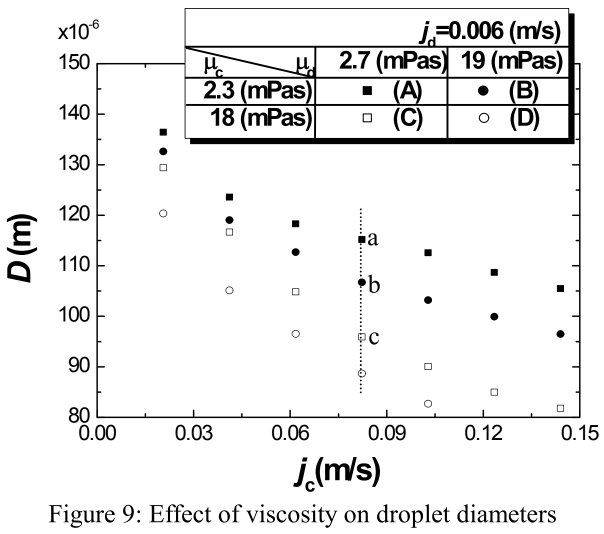

Figure 9: Effect of viscosity on droplet diameters

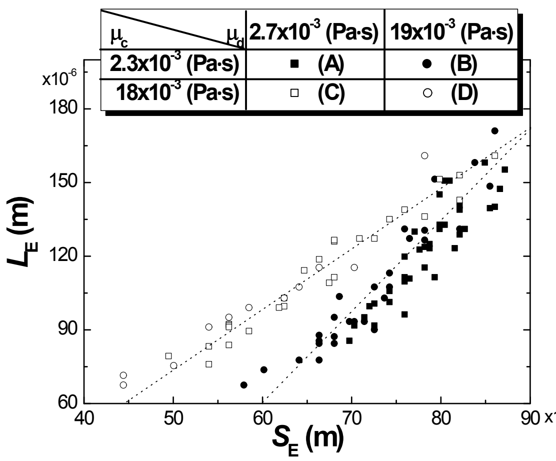

Figure 11: Relationship between L_E and S_E at the end of the X growth stage

be directly correlated to the volume of the formed droplet. Furthermore, L_E appears to be proportional to S_E provided that the viscosity of the continuous phase remains the same, as shown in Figure 11. Therefore, it can be tentatively concluded that D is proportional to S_E and the droplet size at micro T-junction can be estimated by predicting the value of S_E through modeling.

CONCLUSION

In this paper, the phenomenon of the droplet formation at a micro T-junction by dripping is reported. The drop formation process was visualized by using a high speed camera, and the process was classified into the X-Y growth, the X growth, and the detachment stages. The characteristics of each stage were described in detail, and size variation of the bulged part of the disperse phase in Y direction with time was examined.

The formed droplet sizes were measured to provide quantitative data with the viscosity and the superficial velocity of each fluid taken as parameters. The sizes of the micro-droplets generally decrease with a larger superficial velocity of the continuous phase and/or with a smaller superficial velocity of the disperse phase. The droplet size also decreases when the viscosity of the either fluid increases. These phenomena are caused by the increase of the drag force at the interface between the two phases.

Finally, the relationship between the volume of the bulged part at the end of the X growth stage and that of the formed droplets was examined. The results showed that proportional relationships between D^3 and $S_E^2L_E$, and S_E and L_E existed. Hence, it is likely that S_E and D are proportional to each other. Therefore, the modeling of S_E is suggested and it is left as a future work.

ACKNOWLEDGMENTS

This research was supported by Basic Science Research Program through the National Research Foundation of Korea(NRF) funded by the Ministry of Education, Science and Technology (KRF-2008-314-D00045) and also by KAIST (Korea Advanced Institute of Science and Technology).

REFERENCES

1. H. Song, D. L. Chen, and R. F. Ismagilov, 2006, “Reactions in droplets in microfluidic channels,” *Angewandte Chemie International Edition*, Vol. 45, pp. 7336-7356.
2. K. D. Dorfman, M. Chabert, J.-H. Codarbox, G. Rousseau, P. de Cremoux, and J.-L. Viovi, 2005, “Contamination-Free continuous flow microfluidics polymerase chain reaction for quantitative and clinical applications,” *Analytical Chemistry*, Vol. 77, pp. 3700-3704.
3. D. Dendukuri, K. Tsoi, T. A. Hatton, and P. S. Doyle, 2005, “Controlled synthesis of nonspherical microparticles using microfluidics,” *Langmuir*, Vol. 21, pp. 2113-2116.
4. K. Jähnisch, V. Hessel, H. Löwe, and M. Baerns, 2004, “Chemistry in microstructured reactors,” *Angewandte Chemie International Edition*, Vol. 43, pp. 406-446.
5. C. Cramer, P. Fischer, and E. J. Windhab, 2004, “Drop formation in a co-flowing ambient fluid,” *Chemical Engineering Science*, Vol. 59, pp. 3045-3058.
6. S. L. Anna, N. Bontoux, and H. A. Stone, 2003, “Formation of dispersions using flow focusing in microchannels,” *Applied Physics Letters*, Vol. 82, pp. 364-366
7. G. F. Christopher and S. L. Anna, 2007, “Microfluidic methods for generating continuous droplet streams,” *Journal of Physics D: Applied Physics*, Vol. 40, pp.R319-R336.
8. D. Dendukuri and P. S. Doyle, 2009, “The synthesis and assembly of polymeric microparticles using microfluidics,” *Advanced Materials*, Vol. 27, pp.4071-4086.
9. P. Garstecki, M. J. Fuerstman, H. A. Stone, and G. M. Whitesides, 2006, “Formation of droplets and bubbles in a microfluidics T-junction-scaling and mechanism of break-up,” *Lab on a chip*, Vol. 6, pp. 437-446.
10. S. Yeom, 2007, “Microbubbles generation for two-phase flow micromixing,” M. S. Thesis, KAIST, Daejeon, Republic of Korea.
11. M. De Menech, P. Garstecki, F. Jousse, and H. A. Stone, 2008, “Transition from squeezing to dripping in a microfluidics T-shaped junction,” *Journal of Fluid Mechanics*, Vol. 595, pp.141-161.
12. T. Thorsen, R. W. Roberts, F. H. Arnold, and S. R. Quake, 2001, “Dynamic pattern formation in a vesicle-generating microfluidic device,” *Physical Review Letters*, Vol. 86, pp. 4163-4166.
13. S. van der Graaf, T. Nisisako, C. G. P. H. Schroën, R. G. M. van der Sman, and R. M. Boom, 2006, “Lattice Boltzmann simulations of droplet formation in a T-shaped microchannel,” *Langmuir*, Vol. 22, pp. 4144-4152.
14. J. H. Xu, S. W. Li, J. Tan, and G. S. Luo, 2008, “Correlation of droplet formation in T-junction microfluidics devices: From squeezing to dripping,” *Microfluidics and Nanofluidics*, Vol. 5, pp. 711-717.
15. J. Husny and J. J. Cooper-white, 2006, “The effect of elasticity on drop creation in T-shaped microchannels,” *Journal of Non-Newtonian Fluid Mechanics*, Vol. 137, pp. 121-136.
16. J. D. Tice, A. D. Lyon, R. F. Ismagilov, 2004, “Effects of viscosity on droplet formation and mixing in microfluidics channels,” *Analytica Chimica Acta*, Vol. 507, pp. 73-77.
17. M. Oishi, H. Kinoshita, T. Fujii, and M. Oshima, 2009, “Confocal micro-PIV measurement of droplet formation in a T-shaped micro-junction,” *Journal of Physics: Conference Series*, Vol. 146, pp. 012061.
18. R. Clift, J. R. Grace, and M. E. Weber, 1978, “Bubbles, drops, and particles,” Academic Press, Inc.

